THE JOURNAL OF PHYSICAL CHEMISTRY C

Article

Cite This: J. Phys. Chem. C 2017, 121, 24317-24323

pubs.acs.org/JPCC

Charge Transfer-Induced Torsional Dynamics in the Excited State of 2,6-Bis(diphenylamino)anthraquinone

Jungkweon Choi,*[,†,‡] Doo-Sik Ahn,[†,‡] Key Young Oang,[§] Dae Won Cho,[∥] and Hyotcherl Ihee*[,†,‡]

[†]Center for Nanomaterials and Chemical Reactions, Institute for Basic Science, Daejeon 34141, Republic of Korea

[‡]Department of Chemistry, KAIST, Daejeon 34141, Republic of Korea

[§]Radiation Center for Ultrafast Science, Quantum Optics Division, Korea Atomic Energy Research Institute (KAERI), Daejeon 34057, Republic of Korea

[∥]Department of Advanced Materials Chemistry, Korea University, Sejong Campus, Sejong 30019, Korea

Supporting Information

ABSTRACT: Intramolecular charge transfer (ICT) in a multibranched push−pull chromophore is a key photophysical process which is attracting attention due to its relevance to the development of highly efficient organic light-emitting diodes, but the excited-state dynamics of multibranched push−pull chromophores is still unclear. Here, using femtosecond transient absorption spectroscopy and singular value decomposition analysis, we studied the excited state dynamics of 2,6-bis(diphenylamino)anthraquinone (DPA-AQ-DPA), which contains two diphenylamino (DPA) groups as electron-donors (D) and anthraquinone (AQ) as an electron-acceptor (A) and is a candidate for an efficient red TADF (thermally activated delayed fluorescence) emitter. The emission of DPA-AQ-DPA exhibits large Stokes shifts with increasing solvent polarity, indicating that the emission can be attributed to an ICT process. The charge separated (CS) state formed by ICT undergoes torsional dynamics, involving twisting between D and A, resulting in the formation of a twisted charge separated state ($CS_{twisting}$). This twisting reaction between D and A is accelerated in high-polarity solvents compared with that in low-polarity solvents. Such faster CT-induced torsional dynamics in high-polarity solvents is explained in terms of the localization of ICT on one of two ICT branches, suggesting that DPA-AQ-DPA in localized $CS_{twisting}$ formed in high-polarity solvents has two different dihedral angles between a single A group and two D groups. On the other hand, with increasing solvent polarity, the CS and $CS_{twisting}$ states of DPA-AQ-DPA become stabilized, making their energy levels considerably lower than that of $^3(\pi,\pi^*)$, consequently blocking the formation of the triplet excited state and TADF in a high-polarity solvent such as acetonitrile. By contrast, the energy levels of CS and $CS_{twisting}$ states in a low-polarity solvent, such as diethyl ether, are higher than that of $^3(\pi,\pi^*)$, allowing for deactivation into ^{3}DPA-AQ-DPA* through intersystem crossing. This result indicates that the energy levels of CS and $CS_{twisting}$ states can be adjusted by controlling aspects of the local environment, such as solvents, so that intersystem crossing can be either inhibited or promoted. In other words, the energy gap (ΔE_{ST}) between the lowest singlet and triplet excited states for DPA-AQ-DPA can be regulated by changing the solvent polarity.

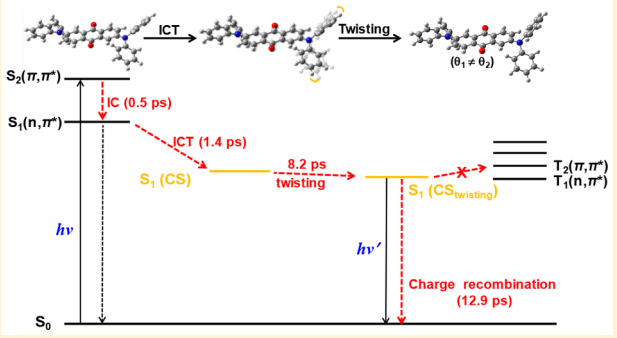

INTRODUCTION

Charge transfer (CT) is an essential process occurring in various biological systems as well as in numerous chemical reactions; therefore, understanding the CT process is critical for regulating the reaction pathway. In this regard, intramolecular CT (ICT) in D−A dyads containing an electron-donor (D) and an electron-acceptor (A) has been extensively investigated with a wide variety of experimental and theoretical approaches.[1−10] The ICT process in D−A dyads is significantly affected by solvent polarity and hydrogen bonding with protic polar solvents, and the molecular geometry in D−A dyads plays an important role in the formation of a charge separated (CS) state in the excited state.[3,6,10,11] Moreover, in high-polarity solvents, it has been shown that many D−A dyads in which D and A units are joined by a single bond undergo twisting in the dihedral angle between D and A groups accompanied by ICT; this results in the formation of a twisted intramolecular charge transfer (TICT) state. Compared to a simple D−A dyad, ICT in multibranched molecules with two or more linear ICT moieties is more complicated. For example, a multibranched push−pull chromophore in a high-polarity solvent tends to exhibit the localization of ICT on one of two or more ICT moieties, whereas simple D−A dyads have been shown to involve delocalized charge separation.

On the other hand, the small energy gap (ΔE_{ST}) between the lowest singlet (S_1) and triplet (T_1) excited states can allow up-conversion from T_1 to S_1 by the absorption of environmental thermal energy, resulting in radiative decay from S_1.[12−16]

Received: July 31, 2017
Revised: September 11, 2017
Published: October 2, 2017

DOI: 10.1021/acs.jpcc.7b07553
J. Phys. Chem. C 2017, 121, 24317−24323

This thermally activated delayed fluorescence (TADF) has been extensively investigated due to its relevance to the development of highly efficient organic light-emitting diodes (OLEDs).[12−21] Recently, it has been shown that many efficient CT complexes including multibranched push−pull chromophores are excellent candidates for TADF emitters because of their high internal quantum efficiencies.[12,15,16,19−21] In particular, ICT emitters with large dihedral angles between D and A groups have been proposed as excellent candidates for efficient blue, green, and red TADF emitters that can improve the output efficiency of optoelectronic devices. Zhang et al. demonstrated that anthraquinone-based ICT compounds, which have a configuration of D-A-D or D-π−A-π-D, exhibit efficient red TADF.[12] However, the excited state dynamics of their CT complexes is still unclear. Here, we investigated the excited state dynamics of 2,6-bis(diphenylamino)anthraquinone (DPA-AQ-DPA), which is a candidate for a red TADF emitter, using femtosecond transient absorption (TA) spectroscopy and kinetics analysis aided by singular value decomposition (SVD). Quinone compounds with a carbonyl group exist in natural photosynthesis systems and play an important role as electron and hydrogen atom acceptors.[22−25] DPA-AQ-DPA, which contains two diphenylamino groups (DPA) as D and one anthraquinone (AQ) as A, can be considered a multibranched molecule with two linear ICT moieties (Figure 1). The results presented in this study reveal

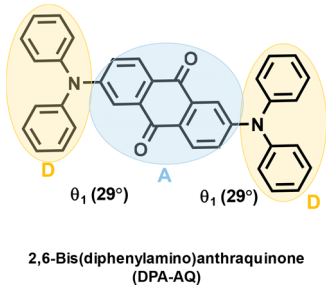

Figure 1. Structure of 2,6-bis(diphenylamino)anthraquinone (DPA-AQ-DPA). The theoretical calculation shows that DPA-AQ-DPA in the ground state has dihedral angles of 29° between D and A groups ($\theta_1 = \theta_2$). (ref 12) The multibranched push−pull chromophore with two or more ICT moieties exhibits either a localized CS state on one of the branches or a delocalized CS state over all of the branches. In this regard, the torsional dynamics induced by a localized CS state on one of the branches may result in the different dihedral angles ($\theta_1 \neq \theta_2$), whereas the torsional dynamics by a delocalized C state over all of the branches leads to the same dihedral angles ($\theta_1 = \theta_2$).

that structural change, such as twisting between DPA and AQ moieties, takes place more slowly than the charge transfer between DPA and AQ. In addition, the faster rate of twisting between D and A in high-polarity solvents is interpreted in terms of localized charge separation, suggesting that the two dihedral angles of DPA-AQ-DPA in a localized $CS_{twisting}$ state are not the same ($\theta_1 \neq \theta_2$). We thoroughly discuss the excited state dynamics of DPA-AQ-DPA and show that the energy gap (ΔE_{ST}) between the lowest singlet (S_1) and triplet excited states for DPA-AQ-DPA can be regulated by changing the solvent polarity.

RESULTS AND DISCUSSION

Figure 2 shows the UV−visible absorption and emission spectra of DPA-AQ-DPA in various solvents. DPA-AQ-DPA shows absorption bands at 370 and 440 nm due to $S_0 \rightarrow S_2(\pi,\pi^*)$ and

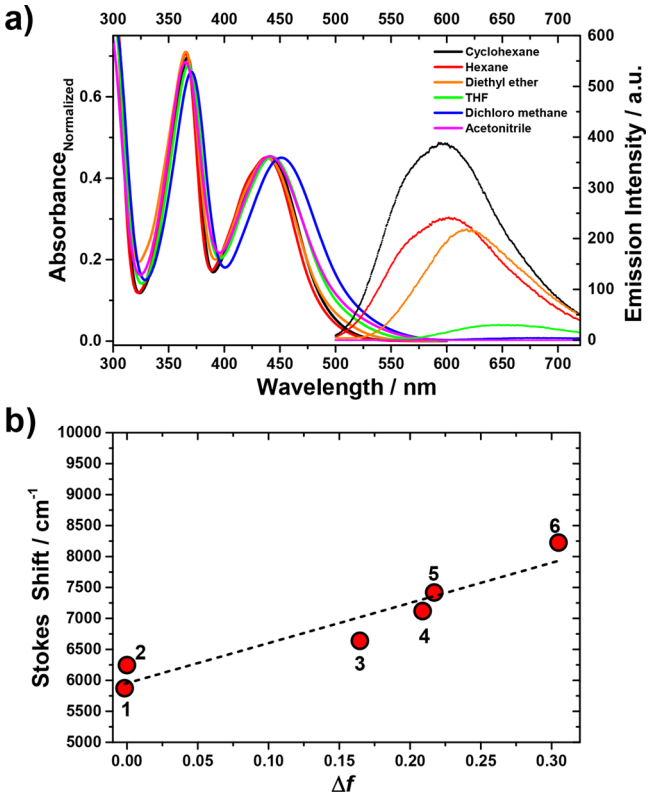

Figure 2. (a) UV−vis absorption and emission spectra of DPA-AQ-DPA measured in various solvents. Excitation wavelength is 370 nm. (b) Lippert−Mataga plot for DPA-AQ-DPA measured in various solvents: 1, cyclohexane; 2, *n*-hexane; 3, diethyl ether; 4, THF; 5, CH_2Cl_2; and 6, MeCN.

$S_0 \rightarrow S_1(n,\pi^*)$ transitions, respectively. The DFT calculation by Zhang et al. shows that the absorption band corresponding to the $S_0 \rightarrow S_1(n,\pi^*)$ transition has a CT character.[12] As shown in Figures 2 and S1, DPA-AQ-DPA exhibits a broad emission band with great dependence on solvent polarity. The emission of DPA-AQ-DPA is weakened and significantly red-shifted as the solvent polarity increases. The Stokes shifts in cyclohexane and acetonitrile (MeCN) are determined to be 5870 and 8230 cm^{-1}, respectively. These large Stokes shifts mean that the emission comes from the CS state. That is, ICT takes place efficiently from DPA to AQ even in nonpolar solvents. To understand the nature of ICT, we plot the Stokes shifts against the orientation polarizability (Δf) using the Lippert−Mataga equation:[26]

$$\bar{\nu}_A - \bar{\nu}_F = \left(\frac{2}{hc}\right)\left(\frac{1}{a_0^3}\right)(\mu_e - \mu_g)^2\left(\frac{\varepsilon - 1}{2\varepsilon + 1} - \frac{n^2 - 1}{2n^2 + 1}\right)$$

$$= \left(\frac{2}{hc}\right)\left(\frac{1}{a_0^3}\right)(\mu_e - \mu_g)^2 \Delta f$$

where $\bar{\nu}_A$ and $\bar{\nu}_F$ are the wavenumbers of absorption and emission, respectively, ε and n are the dielectric constant and refractive index of the solvent, respectively, $\mu_e - \mu_g$ ($\Delta\mu$) is the difference between the dipole moments of the excited and ground states, c is the speed of light, h is Planck's constant, and a_0 is the radius of the Onsager cavity around the fluorophore. As shown in Figure 2b, the Stokes shifts ($\bar{\nu}_A - \bar{\nu}_F$) induced by ICT change linearly with Δf. From the slope of the plot, the $\Delta\mu$ is determined to be 12.7 D. Since the μ_g having a symmetric structure is effectively zero, the μ_e is determined to be 12.7 D. The DFT calculation by Zhang et al. shows that the dihedral

DOI: 10.1021/acs.jpcc.7b07553
J. Phys. Chem. C 2017, 121, 24317−24323

angle between D and A is larger in the excited state than in the ground state,[12] suggesting that a twisting reaction takes place in the excited state. Furthermore, our DFT calculations for DPA-AQ-DPA in diethyl ether and MeCN show similar results (see Tables S1 and S2 and Figure S2). Based on the DFT calculations for DPA-AQ-DPA, we speculated that the large Stokes shifts reflect the twisting reaction of the dihedral angle between D and A induced by ICT.

To further elucidate ICT, we measured the femtosecond TA spectra of DPA-AQ-DPA in diethyl ether and MeCN with 330 nm laser excitation, which corresponds to the π,π^* transition. As shown in Figure S3, the TA spectra of DPA-AQ-DPA in a low-polarity solvent such as diethyl ether consist of a positive signal at 520−750 nm and a negative signal at around 475 nm. The latter is due to the ground state bleach (GSB) of DPA-AQ-DPA. The positive signal at 520−750 nm corresponds to the excited state absorption (ESA) and is blue-shifted in early time-delays. All decay profiles monitored at several wavelengths can be expressed by penta-exponential functions with shared relaxation times of 0.8 ± 0.1 ps, 3.2 ± 0.1 ps, 136 ± 17 ps, 768 ± 8 ps, and >3 ns. The last relaxation time is essentially a constant as we could not precisely determine it because of the limited range of investigated delay times. DPA-AQ-DPA in a high-polarity solvent such as MeCN shows a positive band at 520−750 nm with an absorption maximum at 630 nm and a negative signal at around 475 nm, corresponding to ESA and GSB, respectively (Figure 3). The positive signal at 520−750 nm is blue-shifted in early time-delays. All decay profiles monitored at several wavelengths can be expressed by triexponential functions with shared relaxation times of 0.5 ± 0.1, 2.6 ± 0.1, and 13.5 ± 0.1 ps.

The earliest kinetic component (0.8 and 0.5 ps in diethyl ether and MeCN, respectively) can be interpreted as either fast intersystem crossing (ISC) or internal conversion (IC) from $S_2(\pi,\pi^*)$ state to $S_1(n,\pi^*)$. van Ramesdonk et al.[27] reported that the excited singlet state of 2-substituted AQ is deactivated to the excited triplet state (^{3}AQ*) through ISC with a rate constant of 2.5×10^{12} s^{-1}, which is close to those measured in this study (1.25 and 2.0×10^{12} s^{-1}). However, if the fast dynamics were due to ISC, a very long-lived component (>3 ns) corresponding to the excited triplet state (^{3}DPA-AQ-DPA*) should be observed in both solvents, because the lifetime of the excited triplet state is generally very long (ca. >10^{-5}s). However, as shown in Figure 3, the ESA and GSB signals measured in MeCN decay completely with a time constant of 13.5 ps. This means that the excited state dynamics of DPA-AQ-DPA in MeCN is completely finished within tens of ps, indicating that ISC does not occur in MeCN, a high-polarity solvent. By contrast, as shown in Figure S3, DPA-AQ-DPA in diethyl ether shows a very long component (>3 ns) corresponding to the triplet excited state, implying that ^{3}DPA-AQ-DPA* indeed is formed in a low-polarity solvent, but its time scale is much slower as will be discussed later. Thus, we attribute the fast dynamics (0.8 and 0.5 ps in diethyl ether and MeCN, respectively) to the internal conversion (IC) from $S_2(\pi,\pi^*)$ state to $S_1(n,\pi^*)$. The ISC process will be further discussed later.

On the other hand, the dynamics of a few picoseconds (3.2 and 2.6 ps in diethyl ether and MeCN, respectively) exhibit dependence on solvent polarity and accompany the blue shift of the excited state absorption as depicted in Figures 3 and S3, indicating that these dynamics are related to ICT process. Many CT complexes have shown the following relation:[2]

$$k_{CT} \cong \tau_s^{-1}$$

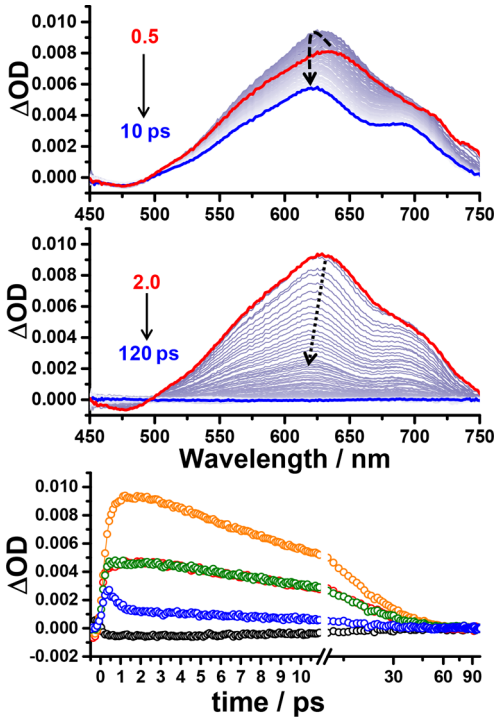

Figure 3. (Top and middle) Transient absorption spectra of DPA-AQ-DPA in MeCN. Excitation wavelength is 330 nm. (Bottom) Decay profiles monitored at selected wavelengths (black circle: 480 nm, red circle: 560 nm, orange circle: 630 nm, green circle: 700 nm, and blue circle: 735 nm).

where k_{CT} and τ_s are the CT rate and the time constant for solvent reorganization, respectively. This relation can be expressed also by $k_{CT} \cong \tau_L^{-1}$, because τ_s is close to τ_L, the longitudinal dielectric relaxation time of the solvent, as predicted by theoretical calculations.[28−31] Kosower and Huppert showed that the ET rate correlates linearly with τ_L^{-1}.[32] Although the time constant of 2.6 ps determined in MeCN is slightly far from the τ_s value of MeCN (0.4−0.9 ps),[33] the dynamics of 3.2 ps observed in diethyl ether is close to the τ_L value of diethyl ether (2 ps).[34] Thus, we attribute this process, which is dependent on the solvent polarity, to ICT. After photoexcitation of DPA-AQ-DPA, CT from DPA to AQ rapidly occurs and results in the formation of an intramolecular charge separated (CS) state.

Finally, the TA spectra measured in diethyl ether and MeCN decay within hundreds and tens of ps, respectively, that is, 136 and 768 ps in diethyl ether and 13.5 ps in MeCN. These relatively slow dynamics compared to the two earliest dynamics attributed to IC and ICT are thought to reflect charge recombination (CR) processes. It is worth noting that, as mentioned above, the CS state of DPA-AQ-DPA in the high-polarity solvent decays completely with a time constant of 13.5 ps without the formation of ^{3}DPA-AQ-DPA*, whereas in the low-polarity solvent, a part of the CS state of DPA-AQ-DPA deactivates to produce ^{3}DPA-AQ-DPA*. Thus, the dynamics of 13.5 ps measured in MeCN can be attributed to the CR process to the ground state, whereas the slow dynamics measured in diethyl ether are related to the CR process to the ground state and the formation of ^{3}DPA-AQ-DPA*. Although it has been proposed that the lowest triplet excited states of AQ and 2-chloro-AQ have a (n,π^*) character,[35,36] ISC can occur only between $^1(n,\pi^*)$ and $^3(\pi,\pi^*)$ because the transition from $^1(n,\pi^*)$ to $^3(n,\pi^*)$ is forbidden by El-Sayed rules. As shown in

DOI: 10.1021/acs.jpcc.7b07553
J. Phys. Chem. C 2017, 121, 24317−24323

Figure 3, the absence of ISC in MeCN suggests that the CS state of DPA-AQ-DPA in a high-polarity solvent is likely to be energetically lower than that of $^3(\pi,\pi^*)$ and there is no TADF process, which in principle can occur because the ISC from CS state to the triplet excited state can be induced through the absorption of environmental thermal energy if ΔE_{ST} between the CS and triplet excited states is small. If such a TADF process occurred, a very long-lived component (>3 ns) corresponding to the triplet excited state (^{3}DPA-AQ-DPA*) should be observed in MeCN, but the data show no triplet−triplet absorption spectrum supporting the formation of ^{3}DPA-AQ-DPA* (see Figure 3). This result indicates that the ISC process from the CS state to the triplet excited state by the absorption of environmental thermal energy does not occur in a high-polarity solvent such as MeCN. Thus, we suggest that the energy level of the CS state in the high-polarity solvent is considerably lower than that of $^3(\pi,\pi^*)$, resulting in the inhibition of ISC and TADF. By contrast, the energy level of the CS state in the low-polarity solvent is higher than that of $^3(\pi,\pi^*)$, leading to efficient ISC to produce ^{3}DPA-AQ-DPA*. For DPA-AQ-DPA in the low-polarity solvent, ISC takes place from $^1(n,\pi^*)$ to $^3(\pi,\pi^*)$, which is not forbidden by the El-Sayed rule. These results indicate that the energy level of the CS state can be adjusted by controlling aspects of the local environment, such as solvents, so that ISC can be either inhibited or promoted. Up to now, most efforts to obtain a small ΔE_{ST} have been devoted to the modification of chemical structures of TADF emitters. However, we show that the energy gap (ΔE_{ST}) between the lowest singlet (S_1) and triplet excited states for DPA-AQ-DPA can be easily regulated by changing the solvent polarity.

As mentioned above, the excited state twisting process of DPA-AQ-DPA in diethyl ether and MeCN was suggested by our DFT calculations (see Table S1). Therefore, we speculated that ICT for DPA-AQ-DPA in both solvents is accompanied by excited state twisting between D and A groups. To further elucidate this, we analyze the spectral relaxation associated with ICT. Most studies on TICT have demonstrated that twisting between D and A groups in the excited state occurs simultaneously with the ICT process. However, several other studies have suggested that structural change, such as twisting between D and A groups, proceeds more slowly than the CT process.[7,37] In this regard, two mechanisms for the TICT reaction in DPA-AQ-DPA, as shown in Figure 4a, need to be considered, namely, the simultaneous (pathway 1) and sequential pathways (pathway 2). Generally, the formation of CS and TICT states can be explained by the spectral shift of the TA spectra because the stabilization of CS and TICT states by interaction with a solvent induces a blue-shift in the TA spectra. Thus, the peak wavelength of the TA spectra for DPA-AQ-DPA in MeCN is plotted as a function of delay times (Figure 4b). The spectral relaxation is well fitted by a biexponential function with two time constants of 1.0 ± 0.3 and 7.9 ± 1.0 ps. The dynamics of 1.0 ps corresponds to the spectral relaxation due to the ICT process from DPA to AQ in the excited state, although the determined time constant of 1.0 ps is slightly different from that determined from decay profiles obtained at specific wavelengths (2.6 ps). Meanwhile, the 7.9 ps time constant is much larger than the τ_s value of MeCN.[33] Therefore, the spectral relaxation occurring with a time constant of 7.9 ps can be interpreted as structural dynamics followed by ICT. According to DFT calculation by Zhang et al.[12] and ours in this work, DPA-AQ-DPA in the excited state has a larger dihedral angle between D and A groups than that in the ground state. In this respect, we

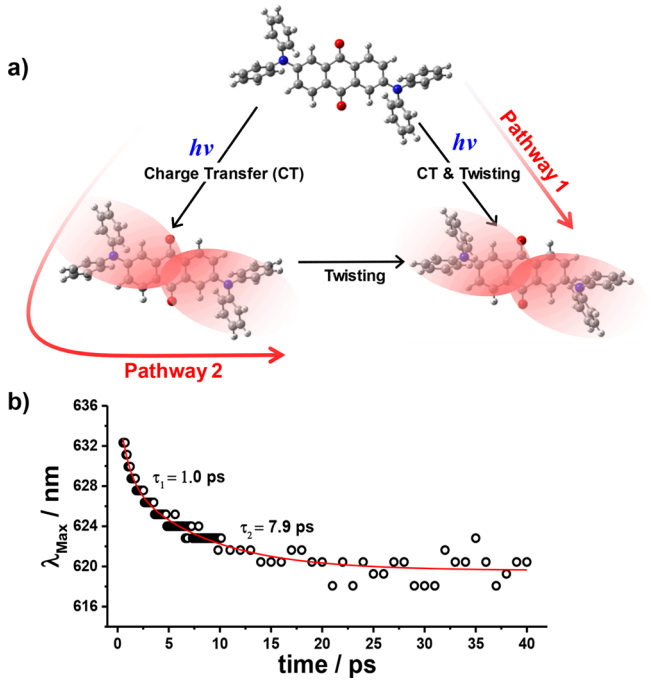

Figure 4. (a) Schematic of twisted intramolecular charge transfer of DPA-AQ-DPA. The red-shaded circles indicate two ICT moieties. (b) Spectral relaxation for DPA-AQ-DPA measured in MeCN. The spectral relaxation is well fitted by the biexponential function with two time constants of 1.0 ± 0.3 and 7.9 ± 1.0 ps. Theoretical fitting curve is shown as red solid line.

attribute the spectral relaxation of 7.9 ps to twisting between DPA and AQ moieties induced by ICT, resulting in the formation of a twisted charge separated state ($CS_{twisting}$).

To confirm the structural dynamics induced by ICT, we analyze the TA spectra for DPA-AQ-DPA in MeCN using SVD and kinetics analysis (see the SI). Up to this point, the decay profiles at several wavelengths in TA data are selected and analyzed to determine the excited-state dynamics of a molecule (in this study, five wavelength points of 480, 560, 630, 700, and 735 nm for DPA-AQ-DPA in MeCN and four wavelength points of 480, 600, 675, and 735 nm for DPA-AQ-DPA in diethyl ether). In contrast, SVD analysis determines the relaxation times associated with all the wavelengths of the measurement (in this study, 255 time delay points in the wavelength range from 450 to 750 nm for DPA-AQ-DPA in MeCN and diethyl ether as well) by simultaneously fitting the principal time-dependent singular components (that is, right singular vectors; rSVs) multiplied by their singular values using a sum of multiple exponentials sharing common relaxation times. Therefore, the relaxation times determined by SVD analysis have a higher global sensitivity but a low local (or wavelength-specific) sensitivity. The SVD analysis for TA spectra of DPA-AQ-DPA in MeCN identifies four significant singular components, indicating the existence of four intermediates. The respective rSVs multiplied by the corresponding singular values fitted by tetra-exponential functions sharing common relaxation times (see Figure S3) show four relaxation times of 0.5 ± 0.1, 1.4 ± 0.4, 8.2 ± 4.2, and 12.9 ± 1.9 ps. The time constant of 1.4 ps determined by spectral relaxation, SVD, and kinetics analysis is close to τ_s values (0.4−0.9 ps) of MeCN. Based on the fit results of the decay profiles obtained at chosen wavelengths and spectral relaxation, four relaxation times of 0.5 ± 0.1, 1.4 ± 0.4, 8.2 ± 4.2, and 12.9 ± 1.9 ps are assigned to

DOI: 10.1021/acs.jpcc.7b07553
J. Phys. Chem. C 2017, 121, 24317−24323

IC, the formation of a CS state via ICT, twisting between D and A to form $CS_{twisting}$, and the CR process to the ground-state, respectively. To confirm our interpretation, we carried out a kinetic analysis using the following reaction scheme:

$$S_0 \xrightarrow{h\nu} S_2(\pi,\pi^*) \xrightarrow{IC} S_1(n,\pi^*) \xrightarrow{ICT} CS \xrightarrow{twisting} CS_{twisting} \xrightarrow{CR} S_0$$

As a result, we found that the excited-state dynamics of DPA-AQ-DPA in the high-polarity solvent is well reproduced by the sequential kinetic model. Figure 5 shows the species-associated spectra and population changes for four intermediates, $S_2(\pi,\pi^*)$, $S_1(n,\pi^*)$, CS state, and $CS_{twisting}$ state. As shown in Figure 5a, ICT occurring with a time constant of

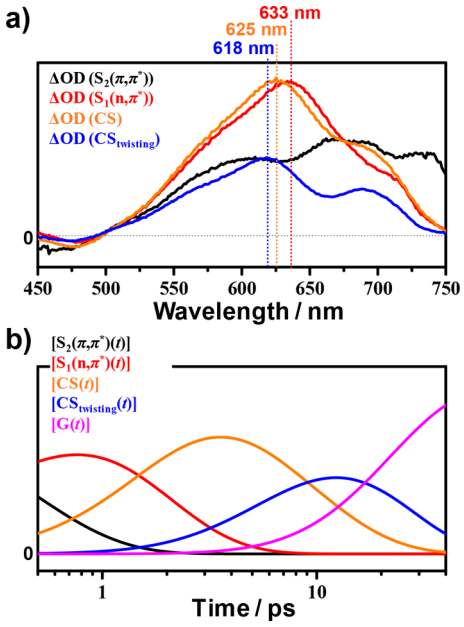

Figure 5. Species-associated spectra (a) and population changes (b) for four intermediates, S_2 (π,π^*), S_1 (n,π^*), CS state, and $CS_{twisting}$ state for DPA-AQ-DPA in MeCM.

1.4 ps induces a spectral blue-shift from 633 to 625 nm. Meanwhile, the twisting in the dihedral angle between D and A occurring with a time constant of 8.2 ps accompanies the spectral blue-shift from 625 to 618 nm. We note that the possibility cannot be ruled out that the torsional dynamics takes place simultaneously with ICT and continues even after ICT is completed.

For the TA spectra of DPA-AQ-DPA in diethyl ether, the SVD analysis shows five significant singular components. From the exponential fit for rSVs multiplied by the corresponding singular values and kinetics analysis, the following reaction scheme of DPA-AQ-DPA in the low-polarity solvent is suggested:

$$S_0 \xrightarrow{h\nu} S_2(\pi,\pi^*) \xrightarrow{IC} S_1(n,\pi^*) \xrightarrow{ICT} CS$$

$$CS \xrightarrow{twisting} CS_{twisting} \xrightarrow{ISC} T_1 \dashrightarrow S_0 \quad (CR: CS_{twisting} \rightarrow S_0)$$

As a result, we determined the five relaxation times of 1.3 ± 0.4 ps, 2.4 ± 0.5 ps, 26 ± 7 ps, 1.3 ± 0.7 ns, and 2.2 ± 0.9 ns, corresponding to IC, the formation of a CS state via ICT, twisting between D and A to form a $CS_{twisting}$ state, ISC to $^3(\pi,\pi^*)$, and the CR process to the ground-state, respectively. Again, we cannot rule out the possibility that the torsional dynamics takes place simultaneously with ICT and continues even after ICT is completed. The time constants of 1.3 and 2.2 ns are different from those (136 and 768 ps) determined from decay profiles monitored at several wavelengths. This difference is probably due to the different analysis method used. As mentioned above, the relaxation times determined by SVD and kinetic analysis have a higher global sensitivity but a low local (or wavelength-specific) sensitivity. Therefore, we explained the excited state dynamics of DPA-AQ-DPA using five time constants determined from SVD analysis.

Here, it is noteworthy that the twisting between D and A occurs even in the low-polarity solvent, diethyl ether. This interpretation is supported by the large Stokes shift observed in diethyl ether (6637 cm^{-1}), DFT calculation by Zhang et al.[12] and ours in this work. Hynes suggested that, although the reaction coordinate for general TICT is the solvent, bianthryl with a pretwisted structure in the ground state can reduce the need for further twisting in the excited state.[38] Therefore, we suggest that the twisting between D and A in the low-polarity solvent is probably facilitated by its pretwisted structure. Furthermore, as shown in Figure S5, the twisting in the dihedral angle between D and A occurring with a time constant of 26 ps accompanies the spectral blue-shift from 680 to 663 nm. The twisting between D and A in diethyl ether with a low viscosity is much slower than in MeCN with a relatively high viscosity ($\tau_{twisting}$ in diethyl ether: 26 ps and $\tau_{twisting}$ in MeCN: 8.2 ps). Generally, torsional dynamics, such as TICT, becomes slow as the solvent viscosity increases. However, the torsional dynamics of DPA-AQ-DPA in the excited state shows the opposite behavior, indicating that the twisting in the dihedral angle between D and A is not influenced by a solvent dynamical frictional effect. Li et al. proposed that the symmetry of multibranched push−pull chromophores is preserved in low-polarity solvents, leading to a delocalized CS state over all of the branches, whereas the symmetry is broken in highly polar solvents, resulting in a localized CS state on one of the branches.[6] In addition, they showed that, in multibranched chromophores, the localization of CS on one of the branches leads to faster solvent-coupled CS state relaxation.[6] Bhaskar et al. also showed that in a multibranched chromophore, the localized CS state in MeCN rapidly decays to a conformationally stabilized CS state, a so-called TICT state.[39] From this point of view, the difference between the torsional dynamics of DPA-AQ-DPA in low-polarity solvents and that in high-polarity solvents can be interpreted by the delocalization/localization of charge separation in DPA-AQ-DPA. That is, the faster rate of twisting between D and A for DPA-AQ-DPA in MeCN is due to the localization of ICT on one of the branches. Based on the delocalization/localization of charge separation in DPA-AQ-DPA, we hypothesize that DPA-AQ-DPA in a localized $CS_{twisting}$ state formed in high-polarity solvents has two different dihedral angles between a single A group and two D groups, whereas DPA-AQ-DPA in a delocalized $CS_{twisting}$ state formed in low-polarity solvents has the same dihedral angles.

On one hand, the rate of ISC for DPA-AQ-DPA in diethyl ether is significantly slower than those for organic aromatic carbonyl compounds.[40−46] For example, the rates of ISC in benzophenone (28 ps in ethanol)[45] and 1-amino-AQ (~10 ps in MeCN)[46] are generally very rapid, resulting in no fluorescence. As shown in Figure 2a, however, DPA-AQ-DPA in the low-polarity solvent shows a moderate emission intensity.

DOI: 10.1021/acs.jpcc.7b07553
J. Phys. Chem. C 2017, 121, 24317−24323

The emission lifetime in diethyl ether is determined to be 3.2 ns (Figure S6), which is close to the rate of CR to S_0 (2.2 ns) within the experimental error. This result implies that the lifetime of the excited singlet state of DPA-AQ-DPA is longer than those of organic aromatic carbonyl compounds, supporting slow ISC.

CONCLUSION

The excited state dynamics of DPA-AQ-DPA has been investigated using femtosecond TA spectroscopy and SVD analysis. The proposed excited state relaxation dynamics for DPA-AQ-DPA in low-polarity and high-polarity solvents are shown in Figure 6 based on the spectral and kinetics analysis.

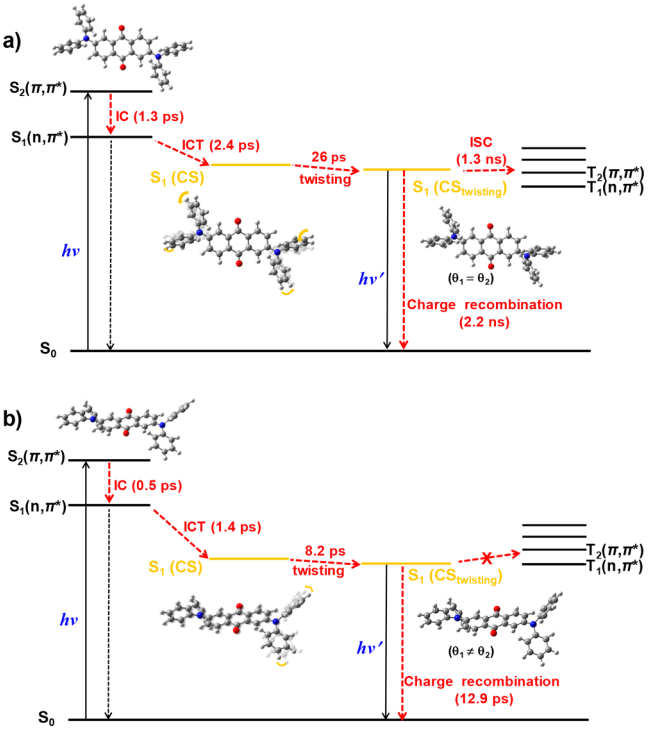

Figure 6. Energy diagram for the charge transfer-induced torsional dynamics in DPA-AQ-DPA in diethyl ether (a) and MeCN (b).

The CS state formed by ICT undergoes torsional dynamics corresponding to the twisting reaction between D and A. This CT-induced torsional dynamics is not influenced by a solvent dynamical friction effect because of the crucial pretwisted structure of DPA-AQ-DPA. Furthermore, the faster rate of twisting between D and A in MeCN is likely due to the localization of ICT on one of the branches. On the other hand, in a high-polarity solvent, such as MeCN, the formation of ^{3}DPA-AQ-DPA* was not observed, indicating that, with increasing solvent polarity, the energy levels of the CS and $CS_{twisting}$ states of DPA-AQ-DPA become low, resulting in a considerably lower energy level in comparison to that of $^3(\pi,\pi^*)$, thereby blocking the ISC process to triplet state and TADF. On the contrary, the energy levels of the $CS_{twisting}$ states of DPA-AQ-DPA in a low-polarity solvent are higher than that of $^3(\pi,\pi^*)$, leading to efficient ISC to produce ^{3}DPA-AQ-DPA*. This result indicates that the energy level of the $CS_{twisting}$ state can be adjusted by means of controlling aspects of the local environment, such as solvents, so that ISC can be either inhibited or promoted. The results presented herein can expand our understanding of the excited state dynamics of CT complexes considered as TADF emitters.

ASSOCIATED CONTENT

Supporting Information

The Supporting Information is available free of charge on the ACS Publications website at DOI: 10.1021/acs.jpcc.7b07553.

Experimental section; TD-DFT and DFT calculated geometric and electronic excitation parameters for S_0 and S_1 ($CS_{twisting}$) in diethyl ether and MeCN; TD-DFT and DFT calculated geometric and electronic excitation parameters for triplet state (T_1) in diethyl ether and MeCN; normalized emission spectra of DPA-AQ-DPA; calculated molecular orbitals for HOMO−1/LUMO and HOMO/LUMO pairs for S_0 and S_1 ($CS_{twisting}$) states, respectively; TA spectra of DPA-AQ-DPA in diethyl ether; SVD analysis TA spectra of DPA-AQ-DPA in MeCN and diethyl ether; emission decay profile of DPA-AQ-DPA in diethyl ether. (PDF)

AUTHOR INFORMATION

Corresponding Authors

*E-mail: jkchoi@ibs.re.kr.
*E-mail: hyotcherl.ihee@kaist.ac.kr.

ORCID

Jungkweon Choi: 0000-0002-9979-305X
Dae Won Cho: 0000-0002-4785-069X
Hyotcherl Ihee: 0000-0003-0397-5965

Notes

The authors declare no competing financial interest.

ACKNOWLEDGMENTS

This work was supported by IBS-R004-A1.

REFERENCES

(1) Su, S. G.; Simon, J. D. Importance of Molecular Size on the Dynamics of Solvent Relaxation. *J. Phys. Chem.* **1989**, *93*, 753−758.
(2) Barbara, P. F.; Walker, G. C.; Smith, T. P. Vibrational Modes and the Dynamic Solvent Effect in Electron and Proton Transfer. *Science* **1992**, *256*, 975−81.
(3) Grabowski, Z. R.; Rotkiewicz, K.; Rettig, W. Structural Changes Accompanying Intramolecular Electron Transfer: Focus on Twisted Intramolecular Charge-Transfer States and Structures. *Chem. Rev.* **2003**, *103*, 3899−4032.
(4) Margulies, E. A.; Miller, C. E.; Wu, Y.; Ma, L.; Schatz, G. C.; Young, R. M.; Wasielewski, M. R. Enabling Singlet Fission by Controlling Intramolecular Charge Transfer in Pi-Stacked Covalent Terrylenediimide Dimers. *Nat. Chem.* **2016**, *8*, 1120−1125.
(5) Escudero, D. Revising Intramolecular Photoinduced Electron Transfer (PET) from First-Principles. *Acc. Chem. Res.* **2016**, *49*, 1816−24.
(6) Li, Y.; Zhou, M.; Niu, Y.; Guo, Q.; Xia, A. Solvent-Dependent Intramolecular Charge Transfer Delocalization/Localization in Multi-branched Push-Pull Chromophores. *J. Chem. Phys.* **2015**, *143*, 034309.
(7) Park, M.; Kim, C. H.; Joo, T. Multifaceted Ultrafast Intramolecular Charge Transfer Dynamics of 4-(Dimethylamino)-Benzonitrile (DMABN). *J. Phys. Chem. A* **2013**, *117*, 370−377.
(8) Kobayashi, M.; Hayakawa, N.; Matsuo, T.; Li, B.; Fukunaga, T.; Hashizume, D.; Fueno, H.; Tanaka, K.; Tamao, K. (Z)-1,2-Di(1-Pyrenyl)Disilene: Synthesis, Structure, and Intramolecular Charge-Transfer Emission. *J. Am. Chem. Soc.* **2016**, *138*, 758−761.
(9) Li, W.; et al. Employing ~ 100% Excitons in Oleds by Utilizing a Fluorescent Molecule with Hybridized Local and Charge-Transfer Excited State. *Adv. Funct. Mater.* **2014**, *24*, 1609−1614.

DOI: 10.1021/acs.jpcc.7b07553
J. Phys. Chem. C 2017, 121, 24317−24323

(10) Cho, Y.-J.; Lee, A.-R.; Kim, S.-Y.; Cho, M.; Han, W.-S.; Son, H.-J.; Cho, D. W.; Kang, S. O. The Influence of π-Conjugation on Competitive Pathways: Charge Transfer or Electron Transfer in New D-π-A and D-π-Si-π-A Dyads. *Phys. Chem. Chem. Phys.* **2016**, *18*, 22921−22928.
(11) Kim, S.-Y.; Cho, Y.-J.; Lee, A.-R.; Son, H.-j.; Han, W.-S.; Cho, D. W.; Kang, S. O. Influence of π-Conjugation Structural Changes on Intramolecular Charge Transfer and Photoinduced Electron Transfer in Donor-π-Acceptor Dyads. *Phys. Chem. Chem. Phys.* **2017**, *19*, 426−435.
(12) Zhang, Q. S.; Kuwabara, H.; Potscavage, W. J.; Huang, S. P.; Hatae, Y.; Shibata, T.; Adachi, C. Anthraquinone-Based Intramolecular Charge-Transfer Compounds: Computational Molecular Design, Thermally Activated Delayed Fluorescence, and Highly Efficient Red Electroluminescence. *J. Am. Chem. Soc.* **2014**, *136*, 18070−18081.
(13) Zhang, Q. S.; Li, B.; Huang, S. P.; Nomura, H.; Tanaka, H.; Adachi, C. Efficient Blue Organic Light-Emitting Diodes Employing Thermally Activated Delayed Fluorescence. *Nat. Photonics* **2014**, *8*, 326−332.
(14) Uoyama, H.; Goushi, K.; Shizu, K.; Nomura, H.; Adachi, C. Highly Efficient Organic Light-Emitting Diodes from Delayed Fluorescence. *Nature* **2012**, *492*, 234−238.
(15) Dias, F. B.; Bourdakos, K. N.; Jankus, V.; Moss, K. C.; Kamtekar, K. T.; Bhalla, V.; Santos, J.; Bryce, M. R.; Monkman, A. P. Triplet Harvesting with 100% Efficiency by Way of Thermally Activated Delayed Fluorescence in Charge Transfer Oled Emitters. *Adv. Mater.* **2013**, *25*, 3707−3714.
(16) Tanaka, H.; Shizu, K.; Nakanotani, H.; Adachi, C. Twisted Intramolecular Charge Transfer State for Long-Wavelength Thermally Activated Delayed Fluorescence. *Chem. Mater.* **2013**, *25*, 3766−3771.
(17) Bell, B. M.; et al. Boron-Based Tadf Emitters with Improved Oled Device Efficiency Roll-Off and Long Lifetime. *Dyes Pigm.* **2017**, *141*, 83−92.
(18) Tsujimoto, H.; Ha, D.-G.; Markopoulos, G.; Chae, H. S.; Baldo, M. A.; Swager, T. M. Thermally Activated Delayed Fluorescence and Aggregation Induced Emission with through-Space Charge Transfer. *J. Am. Chem. Soc.* **2017**, *139*, 4894−4900.
(19) Data, P.; Pander, P.; Okazaki, M.; Takeda, Y.; Minakata, S.; Monkman, A. P. Dibenzo[*a,j*]Phenazine-Cored Donor-Acceptor-Donor Compounds as Green-to-Red/NIR Thermally Activated Delayed Fluorescence Organic Light Emitters. *Angew. Chem., Int. Ed.* **2016**, *55*, 5739−5744.
(20) Dias, F. B.; Penfold, T. J.; Monkman, A. P. Photophysics of Thermally Activated Delayed Fluorescence Molecules. *Methods Appl. Fluoresc.* **2017**, *5*, 012001.
(21) Yang, Z. Y.; Mao, Z.; Xie, Z. L.; Zhang, Y.; Liu, S. W.; Zhao, J.; Xu, J. R.; Chi, Z. G.; Aldred, M. P. Recent Advances in Organic Thermally Activated Delayed Fluorescence Materials. *Chem. Soc. Rev.* **2017**, *46*, 915−1016.
(22) Pritchina, E. A.; Gritsan, N. P.; Burdzinski, G. T.; Platz, M. S. Interplay of Computational Chemistry and Transient Absorption Spectroscopy in the Ultrafast Studies. *J. Struct. Chem.* **2007**, *48*, S55−S63.
(23) Armitage, B.; Yu, C. J.; Devadoss, C.; Schuster, G. B. Cationic Anthraquinone Derivatives as Catalytic DNA Photonucleases - Mechanisms for DNA-Damage and Quinone Recycling. *J. Am. Chem. Soc.* **1994**, *116*, 9847−9859.
(24) Schuster, G. B. Long-Range Charge Transfer in DNA: Transient Structural Distortions Control the Distance Dependence. *Acc. Chem. Res.* **2000**, *33*, 253−260.
(25) Moore, J. N.; Phillips, D.; Hester, R. E. Time-Resolved Resonance Raman-Spectroscopy Applied to the Photochemistry of the Sulfonated Derivatives of 9,10-Anthraquinone. *J. Phys. Chem.* **1988**, *92*, 5619−5627.
(26) Lakowicz, J. R. *Principles of Fluorescence Spectroscopy*, 3rd ed.; Springer US: Singapore, 2010; Chapter 6.
(27) van Ramesdonk, H. J.; Bakker, B. H.; Groeneveld, M. M.; Verhoeven, J. W.; Allen, B. D.; Rostron, J. P.; Harriman, A. Ultrafast Intersystem Crossing in 9,10-Anthraquinones and Intramolecular Charge Separation in an Anthraquinone-Based Dyad. *J. Phys. Chem. A* **2006**, *110*, 13145−13150.
(28) Warshel, A.; Hwang, J. K. Simulation of the Dynamics of Electron-Transfer Reactions in Polar-Solvents - Semiclassical Trajectories and Dispersed Polaron Approaches. *J. Chem. Phys.* **1986**, *84*, 4938−4957.
(29) Sumi, H.; Marcus, R. A. Dynamic Effects in Electron-Transfer Reactions. *J. Chem. Phys.* **1986**, *84*, 4894−4914.
(30) Calef, D. F.; Wolynes, P. G. Classical Solvent Dynamics and Electron-Transfer 0.2. Molecular Aspects. *J. Chem. Phys.* **1983**, *78*, 470−482.
(31) Calef, D. F.; Wolynes, P. G. Classical Solvent Dynamics and Electron-Transfer 0.1. Continuum Theory. *J. Phys. Chem.* **1983**, *87*, 3387−3400.
(32) Kosower, E. M.; Huppert, D. Excited-State Electron and Proton Transfers. *Annu. Rev. Phys. Chem.* **1986**, *37*, 127−156.
(33) Kahlow, M. A.; Kang, T. J.; Barbara, P. F. Electron-Transfer Times Are Not Equal to Longitudinal Relaxation-Times in Polar Aprotic-Solvents. *J. Phys. Chem.* **1987**, *91*, 6452−6455.
(34) Middelhoek, E. R.; van der Meulen, P.; Verhoeven, J. W.; Glasbeek, M. Picosecond Time-Dependent Stokes Shift Studies of Fluoroprobe in Liquid Solution. *Chem. Phys.* **1995**, *198*, 373−380.
(35) Hamanoue, K.; Nakayama, T.; Kajiwara, Y.; Yamaguchi, T.; Teranishi, H. The Lowest Triplet-States of Anthraquinone and Chloroanthraquinones: The 1-Chloro, 2-Chloro, 1,5-Dichloro, and 1,8-Dichloro Compounds. *J. Chem. Phys.* **1987**, *86*, 6654−6659.
(36) Galaup, J. P.; Megel, J.; Trommsdorff, H. P. Assignment of Lowest Triplet-State of 9,10-Anthraquinone Single-Crystals. *Chem. Phys. Lett.* **1976**, *41*, 397−400.
(37) Karunakaran, V.; Das, S. Direct Observation of Cascade of Photoinduced Ultrafast Intramolecular Charge Transfer Dynamics in Diphenyl Acetylene Derivatives: Via Solvation and Intramolecular Relaxation. *J. Phys. Chem. B* **2016**, *120*, 7016−7023.
(38) Hynes, J. T. Twisted Intramolecular Charge Transfer Reactions: The Role of the Solvent. *Rev. Port. Quim.* **1995**, *2*, 12−17.
(39) Bhaskar, A.; Ramakrishna, G.; Lu, Z.; Twieg, R.; Hales, J. M.; Hagan, D. J.; Van Stryland, E.; Goodson, T., 3rd Investigation of Two-Photon Absorption Properties in Branched Alkene and Alkyne Chromophores. *J. Am. Chem. Soc.* **2006**, *128*, 11840−9.
(40) Anderson, R. W.; Hochstrasser, R. M.; Lutz, H.; Scott, G. W. Direct Measurements of Energy-Transfer between Triplet-States of Molecules in Liquids Using Picosecond Pulses. *J. Chem. Phys.* **1974**, *61*, 2500−2506.
(41) Anderson, R. W.; Hochstrasser, R. M.; Lutz, H.; Scott, G. W. Measurements of Intersystem Crossing Kinetics Using 3545-a Picosecond Pulses: Nitronaphthalenes and Benzophenone. *Chem. Phys. Lett.* **1974**, *28*, 153−157.
(42) Damschen, D. E.; Merritt, C. D.; Perry, D. L.; Scott, G. W.; Talley, L. D. Intersystem Crossing Kinetics of Aromatic Ketones in Condensed Phase. *J. Phys. Chem.* **1978**, *82*, 2268−2272.
(43) Hamanoue, K.; Nakayama, T.; Miyake, T.; Teranishi, H. Intersystem Crossing and Lowest Triplet-States of 4-Chromanone, Chromone, and Flavone. *Chem. Lett.* **1981**, *10*, 39−42.
(44) Nakayama, T.; Kuramoto, T.; Hamanoue, K.; Teranishi, H. Absorption Kinetics of Photochemical-Reactions of 2,4,6-Triisopropylbenzophenone and Its Derivatives in Benzene at Room-Temperature Studied by Nanosecond Spectroscopy 0.2. Laser Chemistry, Molecular-Dynamics, Collisions, and Energy-Transfer. *J. Phys. Chem.* **1986**, *90*, 5689−5695.
(45) Aloise, S.; Ruckebusch, C.; Blanchet, L.; Rehault, J.; Buntinx, G.; Huvenne, J. P. The Benzophenone $S_1(n,\pi^*) \rightarrow T_1(n,\pi^*)$ States Intersystem Crossing Reinvestigated by Ultrafast Absorption Spectroscopy and Multivariate Curve Resolution. *J. Phys. Chem. A* **2008**, *112*, 224−231.
(46) Zhang, S.; Sun, S.; Zhou, M.; Wang, L.; Zhang, B. Ultrafast Investigation of Photoinduced Charge Transfer in Aminoanthraquinone Pharmaceutical Product. *Sci. Rep.* **2017**, *7*, 43419.

DOI: 10.1021/acs.jpcc.7b07553
J. Phys. Chem. C 2017, 121, 24317−24323